# Inclusion of cancer-associated fibroblasts in drug screening assays to evaluate pancreatic cancer resistance to therapeutic drugs

**Sarah Brumskill[1,2], Lawrence N Barrera[1], Peter Calcraft[2], Caroline Phillips[2] and Eithne Costello[1*]**

[1] Department of Molecular and Clinical Cancer Medicine, University of Liverpool, Liverpool, UK;
[2] Redx Oncology, Alderley Park, Macclesfield, Cheshire, UK.

**Correspondence:**

Eithne Costello

Institute of Translational Medicine

Department of Clinical Cancer Medicine,

University of Liverpool,

2nd Floor Sherrington Building,

Ashton Street,

Liverpool

L69 3GE

Email: ecostell@liverpool.ac.uk

Telephone: +44 (0)151 795 8032

**Abstract:** Pancreatic ductal adenocarcinoma (PDAC) is characterised by a pro-inflammatory stroma and multi-faceted microenvironment that promotes and maintains tumorigenesis. However, the models used to test new and emerging therapies for PDAC have not increased in complexity to keep pace with our understanding of the human disease. Promising therapies that pass pre-clinical testing often fail in pancreatic cancer clinical trials. The objective of this study was to investigate whether changes in the drug-dosing regimen or the addition of cancer-associated fibroblasts (CAFs) to current existing models can impact the efficacy of chemotherapy drugs used in the clinic. Here, we reveal that gemcitabine and paclitaxel markedly reduce the viability of pancreatic cell lines, but not CAFs, when cultured in 2D. Following the use of an in vitro drug pulsing experiment, PDAC cell lines showed sensitivity to gemcitabine and paclitaxel. However, CAFs were less sensitive to pulsing with gemcitabine compared to their response to paclitaxel. We also identify that a 3D co-culture model of MIA PaCa-2 or PANC-1 with CAFs, showed an increased chemoresistance to gemcitabine when compared to standard 2D mono-cultures a difference to paclitaxel which showed no measurable difference between the 2D and 3D models, suggesting a complex interaction between the drug in study and the cell type used. Changes to standard 2D mono-culture based assays and implementation of 3D co-culture assays, lend complexity to established models and could provide tools for identifying therapies that will match clinically the success observed with in vitro models, thereby aiding in the discovery of novel therapies.

**Keywords:** CAFs; PDAC resistance; drug screening; PDAC chemotherapy

**Key Points**

- For PDAC, the failure rate of drugs tested in phase III clinical trials is high.

- One feature of this cancer is its dense stroma, characterised by a high level of CAFs.

- Addition of CAFs to drug screening models had a marked effect on drug resistance.

- Use of 3D co-culture assays offer tools for ascertaining the efficacy of new drugs.

**Introduction**

Pancreatic cancer is the 4th leading cause of cancer deaths [52] and has an overall 5-year survival of 7-9% [13,48]. Poor survival is due in part to a lack of effective therapies with many clinical trials of potential PDAC treatments failing [6]. A feature of PDAC, which presents a significant barrier to therapeutic intervention is its dense tumour microenvironment [56].

PDAC-associated fibroinflammatory stroma harbours a complex array of activated cancer-associated fibroblasts (CAFs), immune cells, endothelial cells and extracellular matrix proteins such as collagen and fibronectin [42,44,59]. The most abundant cell type in PDAC stroma is CAFs, which were first described in 1998 [2,4]. These cells drive the fibroinflammatory reaction through the deposition of extracellular matrix [20] and the secretion of growth factors and cytokines [19,51]. CAFs also play a significant role in chemoresistance through a variety of mechanisms. For example, the extracellular matrix deposited by CAFs forms a physical barrier to chemotherapy and mediates increased interstitial fluid pressure within the tumour causing impaired vascular function [25]. Additionally, CAFs have been reported to scavenge gemcitabine, a nucleoside analogue, used to treat PDAC, thus reducing the

availability of the drug to cancer cells [23]. They therefore should be considered early in the drug development process in order to maximise the probability of clinical success.

Gemcitabine, was approved for use in metastatic PDAC in 1996 [10,41] and is still used today for the treatment of patients with resectable or advanced PDAC, either as a single agent or in combination with other agents [30,50]. One such other agent is paclitaxel, a microtubule stabilising molecule which has been used to treat many solid tumours. The combination of gemcitabine and nanoparticle albumin–bound paclitaxel (nab-paclitaxel) is a standard of care option for patients with advanced disease [38,57].

The failure rate of drugs tested in phase III clinical trials for PDAC is high, with a large discrepancy between the behaviour of drugs or drug combinations pre-clinically and their performance in randomized control clinical trials [55]. Traditional 2D monolayer-based assays have played a key role in the drug discovery process for decades and are still in use as they provide a cost-effective tool that is fast and easily adapted for high throughput screening strategies [24,36]. Novel organotypic cell culture models and 3D spheroids cultures containing pancreas-derived CAFs have been developed in order to investigate the complex interactions between CAFs and PDAC tumour cells [17,43]. Such models however, have not been incorporated routinely into drug testing programs. Here, we sought to determine whether the inclusion of CAFs to cell-based assays, or whether altering the dosing schedule or the format of the cell culture would affect the ability of gemcitabine paclitaxel to kill PDAC cells in vitro and better reflect clinical efficacy ~~for observations~~. ~~PDAC cells in vitro and better reflect clinical efficacy for observations.~~

## Materials and Methods
### Specimen Collection
Patients with PDAC were selected for this project. Fibrous appearing tissue was selected by the pathologist after a gross analysis of the specimen.

### Isolation of CAFs
CAFs were isolated previously [7] using the outgrowth method [2,4]. This method involves the explantation of pieces of fibrotic tissue removed from the pancreas. Briefly, small pieces of tissue 1mm are arranged in uncoated 6-well tissue culture plates (5-7 pieces/well) and 500μL of Iscove's Modified Dulbecco's Medium (IMDM) supplemented with 20% Fetal Bovine serum (FBS), 2% L-Glutamine and 1% Penicillin Streptomycin was added carefully to ensure that the tissue pieces were not disturbed. Plates were incubated overnight at 37°C in a 5% $CO_2$ air humidified atmosphere. The tissue pieces were removed when fibroblasts reached about 30% confluence. The medium was changed twice weekly using the same medium formulation described above, and cells were grown to 80% confluence, harvested and stored in liquid nitrogen.

### Cell Culture
Cell lines were purchased from the American Type Culture Collection ATCC (MIAPaCa-2, PANC-1, Suit-2, BxPC-3 and AsPC-1). Pancreatic cancer cell lines were cultured in Dulbecco's Modified Eagles Medium (DMEM GlutaMAX) supplemented with 10% FBS. Primary CAFs were recovered from liquid nitrogen simultaneously and placed in a T75 flask with IMDM supplemented with 10% FBS, 2% L-glutamine, and 1% penicillin–streptomycin. Both primary and established cells were incubated at 37°C

in a 5% $CO_2$ air humidified atmosphere. Cells were validated by STR profiling and tested for mycoplasma using e-Myco plus mycoplasma PCR detection kit (iNTRON Biotechnology) following manufacturer instructions.

**Immunofluorescence**

Immunofluorescence (IF) staining was used to stain 2D co-cultures of CAFs and epithelial cancer cell lines. 2D co-cultures CAFs and PANC-1 cells were seeded using IMDM supplemented with 10% FBS, 1% L-glutamine, and 1% penicillin–streptomycin in a 96-well, black, clear bottom, cell carrier plates (PerkinElmer, UK) and left for 24h to adhere; monocultures were also seeded for comparison. The cells were dosed with gemcitabine using a D300 digital liquid dispenser (Tecan). After 72h the media was removed from the plates and the cells were washed twice with PBS ensuring the complete removal of liquid from the wells each time. The cells were fixed with 100μL of 4% PFA per well, for 10min at room temperature before progressing onto the staining protocol. The samples were permeabilised with 0.1% (v/v) Triton X-100 in PBS and incubated for 30min at room temperature. The plates were then washed twice for 5min in PBS and blocked with 5% (v/v) goat serum in PBS for 1h at room temperature before the addition of primary antibodies diluted in blocking solution.

Cells were incubated with primary antibodies (Mouse monoclonal [1A4] to $\alpha$SMA, Rabbit polyclonal to wide spectrum cytokeratin) or isotype controls overnight at 4°C. The following day the antibodies were removed and the plates were washed three times with PBS for 5min each. Secondary antibodies (Goat Anti-Mouse IgG H&L (Alexa Fluor® 488, Goat Anti-Rabbit IgG H&L (Alexa Fluor® 594)) were diluted at 1:500 and incubated for 1h at room temperature. The secondary antibodies were removed and the nuclei were stained with 4', 6-diamidino-2-phenylindole (DAPI) at a 1:10,000 dilution for 10min at room temperature. The plates were then washed 3 times for 5min in PBS. The staining was visualized using an Operetta High-Content Imaging system (PerkinElmer).

Using dual staining within the direct co-cultures it was possible to differentiate cancer cells (CTK stained) from CAFs ($\alpha$SMA stained). Using the isotype controls to remove background fluorescence, it was possible to distinguish $\alpha$SMA positive cells from CTK positive cells. $\alpha$SMA staining was used to determine CAFs which were then subtracted from the total nuclei count. Five regions were imaged in each well at 10x magnification, with each condition run in duplicate. The data was presented as a percentage of the DMSO control.

**Collagen 1a1 ELISA**

CAFs and PDAC cells were seeded in triplicate at a density of 10,000 cells/well in a 12-well plate and after 72h supernatant was harvested and centrifuged at 400g for 5 min to remove cell debris. In order to quantify the collagen1a1 present in the supernatant a Human Pro-Collagen I alpha 1 DuoSet ELISA (R&D Systems) was used following the manufacturer's instructions. Absorbance was measured using an EnVision multilabel plate reader (PerkinElmer) at 450nm.

**2D proliferation assay**

Cells were seeded on a 96-well flat, white, clear bottom plates (Greiner Bio-One) at 1,000 cells/well in 100μL of DMEM-GlutaMAX supplemented with 10% FBS, and left for 24h to adhere. The following day cells were treated with either gemcitabine or paclitaxel using a D300 digital liquid dispenser (Tecan). The plates were placed in an incubator (37°C, 5% $CO_2$) for 72hrs. CellTitre-Glo was prepared using the manufacturer's instructions. At the appropriate time point, plates were removed from the incubator and allowed to equilibrate to room temperature for 30min. 10μL of CellTitre-Glo reagent was added to each well and the plates were sealed with a black plate seal and placed on an orbital shaker for 10min. Luminescence was read using an EnVision plate reader (PerkinElmer). The luminescent signal generated is in direct proportion to the amount of ATP in the well, which is required for the conversion

of luciferin to oxyluciferin in the presence of assay reagents. Cell viability was determined and compared to a DMSO control (0.1%) which was set at 100%.

**Chemotherapy pulsing**

Chemotherapy pulsing was used to determine the effect of mimicking clinical dosing of chemotherapeutic agents in an in vitro assay on the viability of pancreatic cancer cell lines. The cMAX (maximum serum concentration of drug in humans) of gemcitabine (74.4± 11.3 μM) and paclitaxel (4.5± 0.4 μM) [16] was used to calculate an approximate exposure time, such that it matched the total exposure determined by the area under the curve AUC. Once cells had been incubated overnight in order to adhere, the drug was pulsed onto the cells for the length of time each drug is present in serum at a given concentration (Table 1). Once the pulse was completed, media was replaced with fresh vehicle (DMSO) containing media.

**Table 1.** Experimental conditions of chemotherapy pulsing experiment.

| Chemotherapeutic | 0.5 cMAX | | 0.1 cMAX | |
|---|---|---|---|---|
| | Concentration (μM) | Time (min) | Concentration (μM) | Time (min) |
| Gemcitabine | 37.21 | 50 | 7.44 | 250 |
| Paclitaxel | 2.25 | 420 | 0.45 | 2100 |

**Transwell co-culture model**

CAFs and PANC-1 cells (1:1 ratio) were seeded onto a 96-well 0.4μm Transwell plate with 500 CAFs in the lower chamber and 500 PANC-1 in the upper chamber in IMDM supplemented with 10% FBS, 2% L-glutamine, and 1% penicillin–streptomycin. To control for cell number, transwell plates containing PANC-1 cells alone were seeded in both chambers. Cells were incubated for 24h to adhere. The following day they were treated with gemcitabine using a digital liquid dispenser D300 (Tecan). After 72h cell viability of PANC-1 cells was measured using the CellTiter-Glo.

**3D cell culture model**

Cells were seeded, either as a monoculture or co-culture using a 1:1 ratio (500 CAFs: 500 cancer) in Ultra-Low Attachment (ULA) plates at 1000 cells/well and incubated for 24h to form spheroids. The cell number and drug incubation was determined in PANC-1 cells using a cell density gradient assay over a number of time-points (48, 72 and 96h) to determine the most optimal assay conditions. The cells were treated with gemcitabine or paclitaxel and incubated for 72h. The cell viability of 3D spheroids of pancreatic cancer cell lines and/or co-cultures was determined using the Promega 3D CellTiter-Glo assay. Briefly, the CellTiter-Glo 3D reagent was thawed at 4°C overnight and then placed in a 22°C water bath for 30min before use. The plate containing the spheroids was equilibrated for 30min at room temperature. 50μL of CellTiter-Glo 3D was added to each well and placed on an orbital plate shaker for 5 min. The cell lysate and CellTiter-Glo reagent was moved to a flat, clear bottom 96-well plate, incubated for a further 25min (room temperature) and then the luminescent signal was measured using an EnVision multilabel plate reader (Perkin Elmer).

**Statistical analysis**

Statistical tests were performed using GraphPad software V.6.01. Results were considered significant at $P \leq 0.05$.

**Results**

**Gemcitabine and paclitaxel markedly reduce the viability of pancreatic cell lines, but not CAFs, when cultured in 2D.**

CAFs were isolated from PDAC patients using the outgrowth method [2,4] and were shown previously to express the CAF markers, $\alpha$SMA, desmin and vimentin, and to harbour wild-type *KRAS* [7]. In addition, to establish their functionality, we investigated their ability to secrete collagen, a major component of the PDAC microenvironment, which CAFs are responsible for depositing [20]. Conditioned media from three independent CAF isolates (R3088, R3072 and R3134) were evaluated for collagen 1a1 levels by ELISA (Figure 1A). All three isolates secreted considerably more collagen than three established PDAC cell lines tested for comparison (Figure 1A).

We next sought to establish the effects of gemcitabine and paclitaxel on the viability of PDAC cell lines and CAFs in a traditional 2D screening model. Five PDAC cell lines, PANC-1, MIA PaCa-2, Suit-2, AsPC-1 and BxPC-3 showed sub-micromolar sensitivity, in a concentration-dependent manner, to 72h treatment with gemcitabine (Figure 1B). By contrast, CAFs (R3072) were considerably less sensitive to gemcitabine with over 50% of cells remaining viable following exposure to the highest concentration (10μM) of gemcitabine (Figure 1C). Four of the five PDAC cell lines tested (PANC-1, MIA PaCa-2, BxPC3-3 and Suit-2) were more sensitive to paclitaxel treatment (Figure 1D) than CAFs (R3088; Figure 1E). More than 50% (R3088) remained viable following 72h exposure to the highest concentration (10μM) of paclitaxel (Figure 1E). The viability of PDAC cells following 96h exposure to both drugs was determined, with sensitivities to both gemcitabine (Supplementary Figure 1A) and paclitaxel (Supplementary Figure 1B) recorded. Across all of the experimental conditions, the observed potencies to both drugs were in the nM range (Figures 1F and 1G and Supplementary Figures 1C and 1D), with the exception of AsPC-1 cells which showed low sensitivity to paclitaxel after 72h (Figure 1D). Taken together, our data indicate that isolated primary PDAC-associated CAFs retain physiological function, as attested by secretion of collagen, and are resistant to gemcitabine and paclitaxel in a standard 2D monoculture-based assay.

**Chemotherapeutic pulsing as an alternative method for dosing cells in vitro**

Drug screening assays in the pharmaceutical industry are designed with a variety of factors in consideration such as pharmacological relevance, reproducibility, quality and importantly costs [27]. In PDAC research, the standard 2D mono cell-based assay is still the most commonly used method to investigate the effect of chemotherapeutic agents on cancer cells in culture [3,32]. In a 2D mono culture-based assay, chemotherapeutic agents are ranked based on their potency following continuous exposure of cells to a compound. *In vivo* however, the length of time cancer cells are exposed to the drug varies based on a variety of factors, one of which is the rate at which the drug is cleared by the host. In order to investigate whether an *in vitro* dosing schedule which mimics the clinical exposure of cancer cells to the drug would better reflect the *in vivo* performance of the drug, a pulse experiment was

designed. This involved adding the drug for a defined time (pulse), and then removing it for the remaining duration of the experiment. The cMAX values (maximum serum concentration of drug in humans) of gemcitabine (74.4± 11.3µM) and paclitaxel (4.5± 0.4µM) respectively [16] were used to calculate the durations of the pulses such that they matched the total exposure time and concentration determined by the area under the plasma drug concentration curve (AUC) for these agents [16]. The abundant stroma, hypo-vascularity, vascular collapse and high interstitial fluid pressure associated with pancreatic tumours impair drug delivery [45-47]. Dosing using the cMAX would therefore likely overestimate the drug exposure of a pancreatic tumour and consequently 0.5 cMAX and 0.1 cMAX were chosen as a high and low dose respectively of gemcitabine or paclitaxel.

Following gemcitabine treatment (Figure 2A), all of the PDAC cell lines examined showed decreased viability when treated with either 0.1 cMAX (7.44µM; 250 minute pulse) or 0.5 cMAX (37.21µM; 50 minute pulse). MIA PaCa-2 showed the greatest sensitivity when pulsed with gemcitabine in this way, with a statistically significant reduced viability after 72 and 96h compared to the 24h timepoint (P≤0.05). Panc-1 and BxPC-3 also showed a statistically significant reduced viability, while Suit-2 and AsPC-1 showed a similar trend of just under 40% following both 0.1 and 0.5 cMAX at 96 h. By contrast, three independent CAFs analysed (R3088, R3072, R3134) retained resistance to gemcitabine with average cell viability in excess of 60% of the DMSO control at 96 h post dosing (Figure 2B).

PDAC cell lines showed sensitivity to paclitaxel in pulsing experiments (Figure 2C), when treated with 0.1 cMAX (0.45µM for 2100 minutes) and 0.5 cMAX (2.25µM for 420 minutes) with Panc-1 reaching significance, although with the exception of Suit-2 cells, a recovery in cell viability was observed for all PDAC cells at 96 h following treatment with 0.1 cMAX. Compared to their response to gemcitabine, CAFs (R3088, R3072) were more sensitive to pulsing with paclitaxel with cell viability of 35% after 96 h pulsing with both 0.1 cMAX and 0.5 cMAX (Figure 2D).

In summary, under the conditions of *in vitro* drug pulsing, all of the PDAC cell lines showed sensitivity to gemcitabine and paclitaxel. In particular, PDAC cells treated with gemcitabine showed limited signs of recovery within the 96 h experimental timeframe. Given that the partial response rate to gemcitabine of patients with advanced PDAC is 5 to 12% [40,54], we concluded that the use of the *in vitro* drug pulsing protocol on its own is unlikely to minimise the discrepancy between observed effective toxicity *in vitro* and the poor clinical efficacy in patients. This prompted us to investigate alternative *in vitro* models, including the incorporation of CAFs into drug screening assays.

**CAFs reduce the anti-proliferative effect of gemcitabine in 2D co-culture models**

In order to examine whether co-culturing cancer cells with CAFs could influence the sensitivity of the cancer cells to chemotherapeutic agents, we first used a transwell co-culture model, which avoids direct cell-to-cell contact between the two distinct cell types (Figure 3A). Two independent CAF isolates, R3088 and R3072 were evaluated for their effect on the sensitivity of PANC-1 cells to gemcitabine. The presence of R3088 CAFs in the lower chamber of the transwell plate led to a 12.5 fold increase in the $IC_{50}$ (PANC-1 (N=1) IC50 from 14.2nM to 177.5nM) (Figure 3B). Similarly, culturing PANC-1 with R3072 CAFs led to a 22.5 fold increase in the $IC_{50}$ (PANC-1 (N=2) IC50 from 19.1nM to 430.8nM) (Figure 3B). This

suggests that the presence of CAFs reduces the ability of gemcitabine to kill cancer cells and that this effect can occur in the absence of physical contact between CAFs and cancer cells.

We next investigated whether the loss of potency of gemcitabine for PDAC cells would endure if CAFs and cancer cells were grown in a direct co-culture model in the absence of a physical barrier (Figure 3C). Mixed cultures of PANC-1 cells and CAFs (R3088) (Figure 3C), in varying ratios, were treated with gemcitabine for 72 h.  PANC-1 cells and CAFs were then differentiated by fixing and staining with a pan-cytokeratin antibody (pCTK) and an alpha-smooth muscle actin antibody ($\alpha$SMA). The viability of each cell population was determined by counting nuclei associated with distinct areas of positive staining. When compared with a mono-culture of PANC-1 cells, the addition of CAFs reduced the ability of gemcitabine to kill PANC-1 cells (Figure 3D). This occurred regardless of the ratio of PANC-1 cells to CAFs. The exposure of PANC-1 cells alone to gemcitabine resulted in an IC50 of 58nM whereas the addition of CAFs caused a decrease in the sensitivity of PANC-1 to an IC50 of 331nM (PANC-1 to CAF ratio of 9:1); 294nM (PANC-1 to CAF ratio of 1:1); or 437nM (PANC-1 to CAF ratio of 1:9) (Figure 3D).

**CAFs reduce the anti-proliferative effect of gemcitabine in 2D co-culture models**

Next, we sought to evaluate the efficacy of gemcitabine in a 3D co-culture model, which allows for a higher degree of structural complexity in the physical interaction between tumour cells and CAFs, and thus more closely mimics the PDAC tumour microenvironment. 3D models were established by plating cells, either as mono- or co-cultures in Ultra-Low Attachment plates where they formed spheroids (Figure 4A). Responses to gemcitabine under these conditions were compared to a 2D monoculture model (Figure 4A). To determine optimal assay conditions, PANC-1 cells were cultured in 3D using 1,000, 5,000, 10,000, 15,000 and 20,000 cells per well and exposed to a range of concentrations of gemcitabine for 48 h, 72 h, and 96 h (Supplementary Figure 2A). The cell density which gave the optimal assay window using PANC-1 was 1,000 cells/well (Supplementary Figure 2A). However, CAFs (R3088) were found to be minimally sensitive to gemcitabine using the 3D monoculture model (Supplementary Figure 2B). Following the addition of up to 30$\mu$M of this chemotherapeutic agent CAF cell viability did not fall below 69.5% of the DMSO control at the lowest cell density (1,000 cells/well) (Supplementary Figure 2B). The sensitivity of PANC-1 and MIA PaCa-2 cells to gemcitabine decreased when they were cultured in a 3D monoculture model compared to 2D mono-culture (Figure 4B). No difference in the sensitivity of BxPC-3 cells to gemcitabine was observed between these two models (Figure 4B). However curiously, when 2D and 3D mono-cultures of Suit-2 cells were challenged with gemcitabine, the 3D cultures proved to be more sensitive than the 2D cultures.

For 3D co-culture experiments, a ratio of 1:1 PDAC cells to CAFs (R3088) was used as this had been effective in the in-direct and direct 2D co-culture models tested (Figure 3B and Figure 3D). The addition of CAFs to 3D models of PANC1, Suit-2 and BxPC3 was accompanied by greater cell viability, despite the use of concentrations of gemcitabine up to 50$\mu$M. Using 50$\mu$M gemcitabine, the total cell viability of 3D co-cultured CAFs and PANC-1 cells was 90.3% (compared to vehicle-treated controls) versus 33.5% for the PANC1 3D monoculture (compared to vehicle controls).  Similarly, Suit-2 cells in the 3D co-culture model showed a cell viability of 65% when treated with 50 $\mu$M of gemcitabine (compared to vehicle controls) versus 39% at 30$\mu$M gemcitabine in the 3D monoculture, and BxPC3 cells in the 3D co-culture showed a cell viability of 66.6% compared to 33.5% in the 3D monoculture at a concentration of 30$\mu$M gemcitabine. Although using MIA PaCa-2 cells in the 3D co-culture model resulted in variable cell viability, a loss of potency of gemcitabine was nonetheless observed (Figure 4B).

The potency of paclitaxel was also compared in 2D and 3D monoculture in addition to 3D co-culture assays (Supplementary Figure 3). For MIA PaCa-2 cells there was no measurable difference in the potency of paclitaxel between cells cultured in any of the models tested. Similarly, PANC-1 cells showed little change in the IC$_{50}$ values when comparing the three assays. In the case of Suit-2 cells, both the 3D

and 2D monoculture assays gave similar $IC_{50}$ values (7.8 and 3.1 nM respectively). In the Suit-2 3D co-culture assay it was not possible to determine an $IC_{50}$ value due to the shape of the curve, however the cell viability at 100μM paclitaxel was approximately 45% (compared to vehicle control treated cells) versus 32% in the Suit-2 3D monoculture assay at 30μM paclitaxel. It was not possible to determine an $IC_{50}$ value for BxPC3 cells cultured with CAFs in the 3D co-culture model as inhibition of cell viability reached only approximately 70%. Taken together these data provide further evidence that CAFs provide a margin of chemoresistance that is not observed in PDAC cell line mono-cultures and that their incorporation into models in drug discovery deserves further consideration.

**Discussion**

The marked discrepancy between *in vitro* cytotoxicity studies showing effectiveness of gemcitabine or paclitaxel against pancreatic cancer cells [1,8] and *in vivo* or clinical trial studies which show only small survival gains from these chemotherapies [3,11] raises important questions about the reliability of cell based pre-clinical testing. Profiling the anti-proliferative potencies of new therapies using $IC_{50}$ values obtained from 2D monolayer assays [9,37] is well established, inexpensive and reproducible [29,32]. However, limitations include the lack of consideration of dosing schedule and the potential contribution of non-cancer cells of the tumour microenvironment to treatment response. In relation to dosing schedule, we observed that pancreatic cancer cells demonstrated sensitivity to both gemcitabine and paclitaxel in an *in vitro* drug pulsing assay, suggesting that this protocol was unlikely to minimise the discrepancy between observed effective toxicity *in vitro* and poor clinical efficacy. We therefore turned our attention to the incorporation of CAFs into drug screening assays.

We firstly ascertained that CAFs, isolated from three surgically resected PDAC tissue samples, were functionally active as demonstrated by their secretion of collagen 1A1, in agreement with their myofibroblast role in regulating collagen fibres in the tumour microenvironment [5,22]. Unlike PDAC cell lines, our isolated CAFs displayed intrinsic resistance to gemcitabine and paclitaxel, consistent with previous studies in PDAC [49] and in breast and lung cancers [53].

Diminished gemcitabine potency for PDAC cells was observed under all conditions where PDAC and CAFs were co-cultured. Our transwell co-culture model highlighted that physical contact between CAFs and PDAC cells was not a prerequisite for the reduced gemcitabine cytotoxicity. Hessmann et al. similarly observed that conditioned media of murine CAFs pre-incubated with gemcitabine led to a 40-80% increment in the cell viability of KPC cell lines in comparison to fresh addition of gemcitabine to CAF-conditioned media, attributing this effect to gemcitabine scavenging properties of CAFs *in vitro* [23]. Such a fibroblast-dependent protective effect is consistent with the observation that addition of NIH-3T3 fibroblasts to a transwell co-culture with BxPC3 cells reduced the effect of doxorubicin on BxPC3 cells, which could be rescued by the addition of smoothened inhibitor vismodegib indicating that paracrine Hh signalling was active in the co-culture [61]. Taken together this indicates that CAFs provide a chemotherapeutic-resistance mechanism to PDAC cells which is not dependent upon physical contact between CAFs and PDAC cells, suggesting that scavenging of gemcitabine and/or a paracrine signalling pathway are significant contributing factors. This is supported by the observation that paracrine signalling is activated by the CAF secretome which has a role in chemoresistance such as mTOR/4E-BP1 [14] and SDF-1$\alpha$ [60].

Using direct co-culture models, we observed a similar loss of gemcitabine potency when the cells were allowed to form physical connections. Such reduction in potency has also been observed in SW480 colon cancer cells in co-culture with WI-38 fibroblasts in the presence of the WNT/β-catenin signalling inhibitor XAV939 [31]. Cell-cell contact between CAFs and squamous cell carcinoma cells have been found to play a role in the invasion and migration of the tumour cells, through ECM remodelling [18]. This indicates that both paracrine and physical communication between CAFs and tumour cells are important in the tumour microenvironment.

Utilising a 3D co-culture model we found that culturing tumour cells in the presence of CAFs reduced the potency of gemcitabine more than in a 2D or 3D monoculture model. These results are in in agreement with *Lee et al.* who used a microfluidic channel plate to embed co-culture spheroids of pancreatic tumour cell lines and CAFs into a collagen matrix and found that co-cultures resulted in increased drug resistance [34]. In head and neck cancers (HNC) 3D spheroids containing co-cultures of HNC cell lines with CAFs showed greater invasiveness than 3D mono-cultures of HNC cell lines into the fibrin matrix of a 3D cell sheet containing oral keratinocytes, fibroblasts and plasma fibrin. In addition, enhanced resistance to cisplatin and sorafenib was more easily observed in 3D spheroids and CAFs than in 2D models [33].

The loss of potency of paclitaxel was observed in 50% only of the cell lines tested in our 3D co-culture model implying that different mechanisms of CAF-mediated resistance are in place depending on the cancer cell line employed. In support of this notion Marusyk et al., (2016) identified variable levels of resistance to paclitaxel and doxorubicin among different breast cancer cell lines co-cultured with CAFs. However, the protection of carcinoma cells by fibroblasts against a different chemotherapeutic drug, lapatinib, was observed more consistently in all the cell lines studied [39]. With respect to mechanism, PDAC cell lines [15] and ovarian tumour cells [58] treated with conditioned medium from CAFs were shown to have increased resistance to paclitaxel, attributed to the presence of IL-6 secreted by the CAFs which has been found to promote survival in tumour cells. Triple-negative breast cancer cells grown in a 3D co-culture with CAFs showed increased resistance to treatment with paclitaxel. This was found to be due to CXCL12-CXCR4 paracrine signalling between the CAFs and tumour cells resulting in activation of the MAPK/PI3K pathways [21].

Culture conditions impart significant functional characteristics on cells. 3D models have been suggested as the future of pharmacological drug screening assays [28] as they recapitulate some aspects of a tumour such as allowing cells to retain a 3D structure [12], the presence of a nutrient gradient, cell junctions [32] and polarity [35]. In a 3D model the cells have less access to the drugs and undergo changes in cell cycle as well as increased hypoxic conditions. All of these factors have been reported to reduce sensitivity to chemotherapies [29]. In addition, it has been found that 3D cell models which have a density comparable to that of tissue will more accurately predict the response to drugs [26]. The data discussed herein adds further evidence to the importance of culture conditions when testing chemotherapeutic agents.

Collectively, this study provides evidence that the PDAC tumour microenvironment is dynamic in its response to chemotherapeutic agents, and CAFs play a much more elaborate role in chemotherapeutic

resistance than just providing a physical barrier. Models such as the 3D and CAF/PDAC co-culture methods used in this study offer an avenue to bridge that gap between *in vitro* and *in vivo* testing, especially in the case of PDAC in which the interactions between CAFs and tumour cells significantly impact responses to therapy. Future studies should investigate other drugs relevant to pancreatic cancer, such as 5-FU and SN38.

**Authors Contributions**: Author Contributions: Conceptualization, S.B., L.B., P.C., C.P., and E.C.; Formal analysis, S.B., L.B., P.C., C.P., and E.C.; Funding acquisition, C.P., and E.C.; Investigation, S.B.; Methodology, S.B., L.B., P.C., C.P., and E.C.; Project administration, C.P., and E.C.; Resources, L.B., C.P., and E.C; Supervision, L.B., P.C., C.P., and E.C.; Validation, S.B.; Visualization, S.B., L.B., and E.C.; Writing – original draft, S.B., L.B., and E.C.; Writing – review & editing, P.C., C.P. The authors declare that all data were generated in-house and that no paper mill was used

**Compliance with ethical standards**

**Research involving human participants and/or animals:** Pancreatic specimens were obtained from patients undergoing surgery to remove a portion of the pancreas with curative intent following the approval of the UK Health Research Authority in accordance with the Declaration of Helsinki, including ethical approval (London – South East Research Ethics Committee, Ref: 16/LO/1630) and written informed consent, from patients undergoing pancreatic surgery at the Royal Liverpool University Hospital.

**Conflicts of Interest:** The authors declare no conflict of interest.

**References:**

1.	Alber, M. S., Lee, J. J., Huang, J., England, C. G., McNally, L. R., & Frieboes, H. B. (2013). Predictive Modeling of In Vivo Response to Gemcitabine in Pancreatic Cancer. PLoS Computational Biology, 9(9). doi:10.1371/journal.pcbi.1003231

2.	Apte, M. V., Haber, P. S., Applegate, T. L., Norton, I. D., McCaughan, G. W., Korsten, M. A., Pirola, R. C., & Wilson, J. S. (1998). Periacinar stellate shaped cells in rat pancreas: identification, isolation, and culture. Gut, 43(1), 128-133. doi:10.1136/gut.43.1.128

3.	Awasthi, N., Zhang, C., Schwarz, A. M., Hinz, S., Wang, C., Williams, N. S., Schwarz, M. A., & Schwarz, R. E. (2013). Comparative benefits of Nab-paclitaxel over gemcitabine or polysorbate-based docetaxel in experimental pancreatic cancer. Carcinogenesis, 34(10), 2361-2369. doi:10.1093/carcin/bgt227

4.	Bachem, M. G., Schneider, E., Gross, H., Weidenbach, H., Schmid, R. M., Menke, A., Siech, M., Beger, H., Grunert, A., & Adler, G. (1998). Identification, culture, and characterization of pancreatic stellate cells in rats and humans. Gastroenterology, 115(2), 421-432. doi:10.1016/s0016-5085(98)70209-4

5.	Bachem, M. G., Schunemann, M., Ramadani, M., Siech, M., Beger, H., Buck, A., Zhou, S., Schmid-Kotsas, A., & Adler, G. (2005). Pancreatic carcinoma cells induce fibrosis by stimulating proliferation and matrix synthesis of stellate cells. Gastroenterology, 128(4), 907-921. doi:10.1053/j.gastro.2004.12.036

6.      Barati Bagherabad, M., Afzaljavan, F., ShahidSales, S., Hassanian, S. M., & Avan, A. (2019). Targeted therapies in pancreatic cancer: Promises and failures. J Cell Biochem, 120(3), 2726-2741. doi:10.1002/jcb.26284

7.      Barrera, L. N., Evans, A., Lane, B., Brumskill, S., Oldfield, F. E., Campbell, F., Andrews, T., Lu, Z., Perez-Mancera, P. A., Liloglou, T., Ashworth, M., Jalali, M., Dawson, R., Nunes, Q., Phillips, P. A., Timms, J. F., Halloran, C., Greenhalf, W., Neoptolemos, J. P., & Costello, E. (2020). Fibroblasts from distinct pancreatic pathologies exhibit disease-specific properties. Cancer Res. doi:10.1158/0008-5472.CAN-19-3534

8.      Braun, L. M., Lagies, S., Guenzle, J., Fichtner-Feigl, S., Wittel, U. A., & Kammerer, B. (2020). Metabolic Adaptation during nab-Paclitaxel Resistance in Pancreatic Cancer Cell Lines. Cells, 9(5). doi:10.3390/cells9051251

9.      Breslin, S., & O'Driscoll, L. (2013). Three-dimensional cell culture: the missing link in drug discovery. Drug Discov Today, 18(5-6), 240-249. doi:10.1016/j.drudis.2012.10.003

10.     Carmichael, J., Fink, U., Russell, R. C., Spittle, M. F., Harris, A. L., Spiessi, G., & Blatter, J. (1996). Phase II study of gemcitabine in patients with advanced pancreatic cancer. Br J Cancer, 73(1), 101-105. doi:10.1038/bjc.1996.18

11.     Corrie, P. G., Qian, W., Basu, B., Valle, J. W., Falk, S., lwuji, C., Wasan, H., Palmer, D., Scott-Brown, M., Wadsley, J., Arif, S., Bridgewater, J., Propper, D., Gillmore, R., Gopinathan, A., Skells, R., Bundi, P., Brais, R., Dalchau, K., Bax, L., Chhabra, A., Machin, A., Dayim, A., McAdam, K., Cummins, S., Wall, L., Ellis, R., Anthoney, A., Evans, J., Ma, Y. T., Isherwood, C., Neesse, A., Tuveson, D., & Jodrell, D. I. (2020). Scheduling nab-paclitaxel combined with gemcitabine as first-line treatment for metastatic pancreatic adenocarcinoma. British Journal of Cancer, 122(12), 1760-1768. doi:10.1038/s41416-020-0846-2

12.     Costa, E. C., Moreira, A. F., de Melo-Diogo, D., Gaspar, V. M., Carvalho, M. P., & Correia, I. J. (2016). 3D tumor spheroids: an overview on the tools and techniques used for their analysis. Biotechnol Adv, 34(8), 1427-1441. doi:10.1016/j.biotechadv.2016.11.002

13.     CRUK. (2020). Pancreatic cancer mortality (Cancer Research UK). Retrieved from https://www.cancerresearchuk.org/health-professional/cancer-statistics/statistics-by-cancer-type/pancreatic-cancer

14.     Duluc, C., Moatassim-Billah, S., Chalabi-Dchar, M., Perraud, A., Samain, R., Breibach, F., Gayral, M., Cordelier, P., Delisle, M. B., Bousquet-Dubouch, M. P., Tomasini, R., Schmid, H., Mathonnet, M., Pyronnet, S., Martineau, Y., & Bousquet, C. (2015). Pharmacological targeting of the protein synthesis mTOR/4E-BP1 pathway in cancer-associated fibroblasts abrogates pancreatic tumour chemoresistance. EMBO Mol Med, 7(6), 735-753. doi:10.15252/emmm.201404346

15.     Feng, R., Morine, Y., Ikemoto, T., Imura, S., Iwahashi, S., Saito, Y., & Shimada, M. (2018). Nab-paclitaxel interrupts cancer-stromal interaction through C-X-C motif chemokine 10-mediated interleukin-6 downregulation in vitro. Cancer Science, 109(8), 2509-2519. doi:10.1111/cas.13694

16.     Fogli, S., Danesi, R., Gennari, A., Donati, S., Conte, P. F., & Del Tacca, M. (2002). Gemcitabine, epirubicin and paclitaxel: pharmacokinetic and pharmacodynamic interactions in advanced breast cancer. Ann Oncol, 13(6), 919-927. doi:10.1093/annonc/mdf164

17.     Froeling, F. E., Marshall, J. F., & Kocher, H. M. (2010). Pancreatic cancer organotypic cultures. J Biotechnol, 148(1), 16-23. doi:10.1016/j.jbiotec.2010.01.008

18.     Gaggioli, C., Hooper, S., Hidalgo-Carcedo, C., Grosse, R., Marshall, J. F., Harrington, K., & Sahai, E. (2007). Fibroblast-led collective invasion of carcinoma cells with differing roles for RhoGTPases in leading and following cells. Nat Cell Biol, 9(12), 1392-1400. doi:10.1038/ncb1658

19. Gorchs, L., Fernandez Moro, C., Bankhead, P., Kern, K. P., Sadeak, I., Meng, Q., Rangelova, E., & Kaipe, H. (2019). Human Pancreatic Carcinoma-Associated Fibroblasts Promote Expression of Co-inhibitory Markers on CD4(+) and CD8(+) T-Cells. Front Immunol, 10, 847. doi:10.3389/fimmu.2019.00847

20. Haber, P. S., Keogh, G. W., Apte, M. V., Moran, C. S., Stewart, N. L., Crawford, D. H., Pirola, R. C., McCaughan, G. W., Ramm, G. A., & Wilson, J. S. (1999). Activation of pancreatic stellate cells in human and experimental pancreatic fibrosis. Am J Pathol, 155(4), 1087-1095. doi:10.1016/S0002-9440(10)65211-X

21. Ham, S. L., Thakuri, P. S., Plaster, M., Li, J., Luker, K. E., Luker, G. D., & Tavana, H. (2018). Three-dimensional tumor model mimics stromal - breast cancer cells signaling. Oncotarget, 9(1), 249-267. doi:10.18632/oncotarget.22922

22. Hanley, C. J., Noble, F., Ward, M., Bullock, M., Drifka, C., Mellone, M., Manousopoulou, A., Johnston, H. E., Hayden, A., Thirdborough, S., Liu, Y., Smith, D. M., Mellows, T., Kao, W. J., Garbis, S. D., Mirnezami, A., Underwood, T. J., Eliceiri, K. W., & Thomas, G. J. (2016). A subset of myofibroblastic cancer-associated fibroblasts regulate collagen fiber elongation, which is prognostic in multiple cancers. Oncotarget, 7(5), 6159-6174. doi:10.18632/oncotarget.6740

23. Hessmann, E., Patzak, M. S., Klein, L., Chen, N., Kari, V., Ramu, I., Bapiro, T. E., Frese, K. K., Gopinathan, A., Richards, F. M., Jodrell, D. I., Verbeke, C., Li, X., Heuchel, R., Lohr, J. M., Johnsen, S. A., Gress, T. M., Ellenrieder, V., & Neesse, A. (2018). Fibroblast drug scavenging increases intratumoural gemcitabine accumulation in murine pancreas cancer. Gut, 67(3), 497-507. doi:10.1136/gutjnl-2016-311954

24. Horvath, P., Aulner, N., Bickle, M., Davies, A. M., Nery, E. D., Ebner, D., Montoya, M. C., Ostling, P., Pietiainen, V., Price, L. S., Shorte, S. L., Turcatti, G., von Schantz, C., & Carragher, N. O. (2016). Screening out irrelevant cell-based models of disease. Nat Rev Drug Discov, 15(11), 751-769. doi:10.1038/nrd.2016.175

25. Hosein, A. N., Brekken, R. A., & Maitra, A. (2020). Pancreatic cancer stroma: an update on therapeutic targeting strategies. Nat Rev Gastroenterol Hepatol. doi:10.1038/s41575-020-0300-1

26. Hsieh, C. H., Chen, Y. D., Huang, S. F., Wang, H. M., & Wu, M. H. (2015). The effect of primary cancer cell culture models on the results of drug chemosensitivity assays: the application of perfusion microbioreactor system as cell culture vessel. Biomed Res Int, 2015, 470283. doi:10.1155/2015/470283

27. Hughes, J. P., Rees, S., Kalindjian, S. B., & Philpott, K. L. (2011). Principles of early drug discovery. Br J Pharmacol, 162(6), 1239-1249. doi:10.1111/j.1476-5381.2010.01127.x

28. Jensen, C., & Teng, Y. (2020). Is It Time to Start Transitioning From 2D to 3D Cell Culture? Front Mol Biosci, 7, 33. doi:10.3389/fmolb.2020.00033

29. Kapalczynska, M., Kolenda, T., Przybyla, W., Zajaczkowska, M., Teresiak, A., Filas, V., Ibbs, M., Blizniak, R., Luczewski, L., & Lamperska, K. (2018). 2D and 3D cell cultures - a comparison of different types of cancer cell cultures. Arch Med Sci, 14(4), 910-919. doi:10.5114/aoms.2016.63743

30. Kleeff, J., Korc, M., Apte, M., La Vecchia, C., Johnson, C. D., Biankin, A. V., Neale, R. E., Tempero, M., Tuveson, D. A., Hruban, R. H., & Neoptolemos, J. P. (2016). Pancreatic cancer. Nat Rev Dis Primers, 2, 16022. doi:10.1038/nrdp.2016.22

31. Koh, B., Jeon, H., Kim, D., Kang, D., & Kim, K. R. (2019). Effect of fibroblast co-culture on the proliferation, viability and drug response of colon cancer cells. Oncol Lett, 17(2), 2409-2417. doi:10.3892/ol.2018.9836

32. Langhans, S. A. (2018). Three-Dimensional in Vitro Cell Culture Models in Drug Discovery and Drug Repositioning. Front Pharmacol, 9, 6. doi:10.3389/fphar.2018.00006

33. Lee, J., Shin, D., & Roh, J. L. (2018). Development of an in vitro cell-sheet cancer model for chemotherapeutic screening. Theranostics, 8(14), 3964-3973. doi:10.7150/thno.26439

34. Lee, J. H., Kim, S. K., Khawar, I. A., Jeong, S. Y., Chung, S., & Kuh, H. J. (2018). Microfluidic co-culture of pancreatic tumor spheroids with stellate cells as a novel 3D model for investigation of stroma-mediated cell motility and drug resistance. J Exp Clin Cancer Res, 37(1), 4. doi:10.1186/s13046-017-0654-6

35. Lelievre, S. A., Kwok, T., & Chittiboyina, S. (2017). Architecture in 3D cell culture: An essential feature for in vitro toxicology. Toxicol In Vitro, 45(Pt 3), 287-295. doi:10.1016/j.tiv.2017.03.012

36. Lovitt, C. J., Shelper, T. B., & Avery, V. M. (2014). Advanced cell culture techniques for cancer drug discovery. Biology (Basel), 3(2), 345-367. doi:10.3390/biology3020345

37. Lv, D., Hu, Z., Lu, L., Lu, H., & Xu, X. (2017). Three-dimensional cell culture: A powerful tool in tumor research and drug discovery. Oncol Lett, 14(6), 6999-7010. doi:10.3892/ol.2017.7134

38. Ma, W. W., & Hidalgo, M. (2013). The winning formulation: the development of paclitaxel in pancreatic cancer. Clin Cancer Res, 19(20), 5572-5579. doi:10.1158/1078-0432.CCR-13-1356

39. Marusyk, A., Tabassum, D. P., Janiszewska, M., Place, A. E., Trinh, A., Rozhok, A. I., Pyne, S., Guerriero, J. L., Shu, S., Ekram, M., Ishkin, A., Cahill, D. P., Nikolsky, Y., Chan, T. A., Rimawi, M. F., Hilsenbeck, S., Schiff, R., Osborne, K. C., Letai, A., & Polyak, K. (2016). Spatial Proximity to Fibroblasts Impacts Molecular Features and Therapeutic Sensitivity of Breast Cancer Cells Influencing Clinical Outcomes. Cancer Research, 76(22), 6495-6506. doi:10.1158/0008-5472.Can-16-1457

40. Min, Y. J., Joo, K. R., Park, N. H., Yun, T. K., Nah, Y. W., Nam, C. W., & Park, J. H. (2002). Gemcitabine therapy in patients with advanced pancreatic cancer. Korean J Intern Med, 17(4), 259-262. doi:10.3904/kjim.2002.17.4.259

41. Moore, M. (1996). Activity of gemcitabine in patients with advanced pancreatic carcinoma. A review. Cancer, 78(3 Suppl), 633-638. doi:10.1002/(SICI)1097-0142(19960801)78:3<633::AID-CNCR44>3.0.CO;2-X

42. Neesse, A., Algul, H., Tuveson, D. A., & Gress, T. M. (2015). Stromal biology and therapy in pancreatic cancer: a changing paradigm. Gut, 64(9), 1476-1484. doi:10.1136/gutjnl-2015-309304

43. Norberg, K. J., Liu, X., Fernández Moro, C., Strell, C., Nania, S., Blümel, M., Balboni, A., Bozóky, B., Heuchel, R. L., & Löhr, J. M. (2020). A novel pancreatic tumour and stellate cell 3D co-culture spheroid model. BMC Cancer, 20(1). doi:10.1186/s12885-020-06867-5

44. Olive, K. P. (2015). Stroma, Stroma Everywhere (Far More Than You Think). Clin Cancer Res, 21(15), 3366-3368. doi:10.1158/1078-0432.CCR-15-0416

45. Olive, K. P., Jacobetz, M. A., Davidson, C. J., Gopinathan, A., McIntyre, D., Honess, D., Madhu, B., Goldgraben, M. A., Caldwell, M. E., Allard, D., Frese, K. K., Denicola, G., Feig, C., Combs, C., Winter, S. P., Ireland-Zecchini, H., Reichelt, S., Howat, W. J., Chang, A., Dhara, M., Wang, L., Ruckert, F., Grutzmann, R., Pilarsky, C., Izeradjene, K., Hingorani, S. R., Huang, P., Davies, S. E., Plunkett, W., Egorin, M., Hruban, R. H., Whitebread, N., McGovern, K., Adams, J., Iacobuzio-Donahue, C., Griffiths, J., & Tuveson, D. A. (2009). Inhibition of Hedgehog signaling enhances delivery of chemotherapy in a mouse model of pancreatic cancer. Science, 324(5933), 1457-1461. doi:1171362 [pii]
10.1126/science.1171362

46. Provenzano, P. P., Cuevas, C., Chang, A. E., Goel, V. K., Von Hoff, D. D., & Hingorani, S. R. (2012). Enzymatic targeting of the stroma ablates physical barriers to treatment of pancreatic ductal adenocarcinoma. Cancer Cell, 21(3), 418-429. doi:10.1016/j.ccr.2012.01.007

47. Provenzano, P. P., & Hingorani, S. R. (2013). Hyaluronan, fluid pressure, and stromal resistance in pancreas cancer. Br J Cancer, 108(1), 1-8. doi:10.1038/bjc.2012.569

48. Rawla, P., Sunkara, T., & Gaduputi, V. (2019). Epidemiology of Pancreatic Cancer: Global Trends, Etiology and Risk Factors. World J Oncol, 10(1), 10-27. doi:10.14740/wjon1166

49. Richards, K. E., Zeleniak, A. E., Fishel, M. L., Wu, J., Littlepage, L. E., & Hill, R. (2017). Cancer-associated fibroblast exosomes regulate survival and proliferation of pancreatic cancer cells. Oncogene, 36(13), 1770-1778. doi:10.1038/onc.2016.353

50. Roth, M. T., Cardin, D. B., & Berlin, J. D. (2020). Recent advances in the treatment of pancreatic cancer. F1000Res, 9. doi:10.12688/f1000research.21981.1

51. Sherman, M. H., Yu, R. T., Tseng, T. W., Sousa, C. M., Liu, S., Truitt, M. L., He, N., Ding, N., Liddle, C., Atkins, A. R., Leblanc, M., Collisson, E. A., Asara, J. M., Kimmelman, A. C., Downes, M., & Evans, R. M. (2017). Stromal cues regulate the pancreatic cancer epigenome and metabolome. Proc Natl Acad Sci U S A, 114(5), 1129-1134. doi:10.1073/pnas.1620164114

52. Siegel, R. L., Miller, K. D., & Jemal, A. (2019). Cancer statistics, 2019. CA Cancer J Clin, 69(1), 7-34. doi:10.3322/caac.21551

53. Sonnenberg, M., van der Kuip, H., Haubeis, S., Fritz, P., Schroth, W., Friedel, G., Simon, W., Murdter, T. E., & Aulitzky, W. E. (2008). Highly variable response to cytotoxic chemotherapy in carcinoma-associated fibroblasts (CAFs) from lung and breast. BMC Cancer, 8, 364. doi:10.1186/1471-2407-8-364

54. Terashima, T., Yamashita, T., Sakai, A., Ohta, H., Hinoue, Y., Toya, D., Kawai, H., Yonejima, M., Urabe, T., Noda, Y., Mizukoshi, E., & Kaneko, S. (2018). Treatment patterns and outcomes of unresectable pancreatic cancer patients in real-life practice: a region-wide analysis. Jpn J Clin Oncol, 48(11), 966-973. doi:10.1093/jjco/hyy132

55. Thota, R., Maitra, A., & Berlin, J. D. (2017). Preclinical Rationale for the Phase III Trials in Metastatic Pancreatic Cancer: Is Wishful Thinking Clouding Successful Drug Development for Pancreatic Cancer? Pancreas, 46(2), 143-150. doi:10.1097/MPA.0000000000000753

56. Uzunparmak, B., & Sahin, I. H. (2019). Pancreatic cancer microenvironment: a current dilemma. Clin Transl Med, 8(1), 2. doi:10.1186/s40169-019-0221-1

57. Von Hoff, D. D., Ervin, T., Arena, F. P., Chiorean, E. G., Infante, J., Moore, M., Seay, T., Tjulandin, S. A., Ma, W. W., Saleh, M. N., Harris, M., Reni, M., Dowden, S., Laheru, D., Bahary, N., Ramanathan, R. K., Tabernero, J., Hidalgo, M., Goldstein, D., Van Cutsem, E., Wei, X., Iglesias, J., & Renschler, M. F. (2013). Increased survival in pancreatic cancer with nab-paclitaxel plus gemcitabine. N Engl J Med, 369(18), 1691-1703. doi:10.1056/NEJMoa1304369

58. Wang, L., Zhang, F., Cui, J. Y., Chen, L., Chen, Y. T., & Liu, B. W. (2018). CAFs enhance paclitaxel resistance by inducing EMT through the IL-6/JAK2/STAT3 pathway. Oncol Rep, 39(5), 2081-2090. doi:10.3892/or.2018.6311

59. Whatcott, C. J., Diep, C. H., Jiang, P., Watanabe, A., LoBello, J., Sima, C., Hostetter, G., Shepard, H. M., Von Hoff, D. D., & Han, H. (2015). Desmoplasia in Primary Tumors and Metastatic Lesions of Pancreatic Cancer. Clin Cancer Res, 21(15), 3561-3568. doi:10.1158/1078-0432.CCR-14-1051

60. Zhang, H., Wu, H., Guan, J., Wang, L., Ren, X., Shi, X., Liang, Z., & Liu, T. (2015). Paracrine SDF-1alpha signaling mediates the effects of PSCs on GEM chemoresistance through an IL-6 autocrine loop in pancreatic cancer cells. Oncotarget, 6(5), 3085-3097. doi:10.18632/oncotarget.3099

61. Zhou, Q., Zhou, Y., Liu, X., & Shen, Y. (2017). GDC-0449 improves the antitumor activity of nano-doxorubicin in pancreatic cancer in a fibroblast-enriched microenvironment. Sci Rep, 7(1), 13379. doi:10.1038/s41598-017-13869-0

**Figure Legends:**

**Figure 1.** Isolated CAFs secrete collagen and are insensitive to gemcitabine and paclitaxel treatments compared to pancreatic cancer cell lines in standard 2D culture conditions. **(A)** Col1a1 secretion from three established pancreatic cancer cell lines and CAFs isolated from three different patients (R3072, R3088 and R3134) was determined by ELISA. The level of Col1a1 secreted by the cancer cell lines was below the acceptable limit of detection for the assay, precluding statistical analysis. **(B-E)** Dose-response curves following gemcitabine treatment of pancreatic cancer cell lines **(B)** and CAFs (R3072) **(C)** or paclitaxel treatment of pancreatic cancer cell lines **(D)** and CAFs (R3088) **(E).** Cells were exposed to increasing concentrations of gemcitabine or paclitaxel and cell viability measured at 72h using CellTiter-Glo. Data were fitted to a sigmoidal dose response curve and IC50 was determined using GraphPad prism. For PDAC cell lines the data are representative of three independent experiments ±SD performed in triplicate and normalised to a DMSO control set to 100%. For CAFs the data are representative of three independent experiments using three biological replicates (R3088, R3072 and R3134) ±SD performed each in triplicate and normalised to a DMSO control set to 100%. **(F-G)** Graphs depicting the mean pIC$_{50}$ in molar (M) ±S.E.M for multiple assays of gemcitabine and paclitaxel in pancreatic cancer cell lines.

**Figure 2.** Chemotherapeutic pulsing with gemcitabine and paclitaxel to mimic clinical dosing *in vitro*. **(A and C)** The graphs show the cell viability of pancreatic cancer cell lines after a pulse with gemcitabine **(A)** or paclitaxel **(C)** representing 0.5cMAX or 0.1cMAX, data was analysed using DMSO as a control set to 100%. **(B and D)** The graphs show the cell viability of CAFs after a pulse with gemcitabine **(B)** or paclitaxel **(D)** representing 0.5cMAX or 0.1cMAX. At 24, 48, 72 and 96h cell viability was determined using CellTiter-Glo. The data are shown as ±S.E.M of at least 2 independent experiments performed in triplicate and normalised to a DMSO control set to 100%. *P* value determined by one-way ANOVA with post hoc Dunnett's test. The * symbol refers to the 0.5 cMAX condition with *$P \leq 0.05$ and **0.01. The Φ symbol refers to the 0.1 cMAX condition with Φ *$P \leq 0.05$.

**Figure 3.** The addition of CAFs to 2D screening models reduces the anti-proliferative effect of gemcitabine on PANC-1 cells. **(A)** Schematic representation of a transwell co-culture model in which the two cell populations are separated by a physical barrier. In this model CAFs were placed in the bottom chamber and PANC-1 cells were on the transwell insert (1:1 ratio). **(B)** Dose-response curve showing the efficacy of gemcitabine in killing PANC-1 cells in a transwell co-culture model of CAFs and PANC-1 cells. Cells were cultured for 72h in the presence of gemcitabine. The cell viability of PANC-1 cells was measured using CellTiter-Glo. The data are shown as mean ±SD of one assay for two CAFs (R3088 and R3072) and normalised to a DMSO control set to 100%. **(C)** Schematic representation of the direct 2D co-culture model with an image depicting anti-αSMA-488 labelled CAFs (Green), anti-CTK-594-labelled PANC-1 cells (Yellow) and nuclei (Blue). The average nuclei count was measured using an Operetta (PerkinElmer), counting 4 randomly assigned areas of interest/well. **(D)** Dose-response curve showing the direct 2D cell viability assay using three different ratios of CAF to PANC-1 cells compared to PANC-1 cells alone. Cells were exposed to gemcitabine and DMSO as control. At 72h cells viability was determined by counting nuclei which were associated with positive pCTK staining (considered PANC1 cells) and which were not associated with areas of positive αSMA staining (considered CAFs). The data are shown as mean ±SD of one assay performed in triplicate.

**Figure 4.** The addition of CAFs to a 3D co-culture model of pancreatic cancer cell lines confers resistance to gemcitabine. **(A)** Schematic representation of the assay formats utilised; a 2D standard monoculture cell viability assay, a 3D monoculture assay of pancreatic cancer cell lines and a 3D co-culture assay of pancreatic cancer cell lines combined with CAFs (R3008). **(B)** Dose-response curves of the different assay formats described above which were treated with various concentrations of gemcitabine. At 72h cell viability was determined using CellTiter-Glo. The data are shown as ±SD of one assay performed in triplicate and normalised to a DMSO control set to 100%.

**Supplementary Figure Legends:**

**Supplementary Figure 1.** Pancreatic cancer cell lines were sensitive to gemcitabine and paclitaxel in standard 2D culture conditions after 96h treatment **(A and B)** Dose-response curve of a 2D cell viability assay. Pancreatic cancer cell lines are sensitive to gemcitabine **(A)** and paclitaxel **(B)**. Cells were exposed to increasing concentrations of gemcitabine or paclitaxel, and cell viability measured at 96h using CellTiter-Glo. Data were fitted to a sigmoidal dose response curve and IC50 was determined using GraphPad prism. The data are shown as ±SD of one assay performed in triplicate and normalised to a DMSO control set to 100%. **(C and D)** Graphs depicting a comparison of the mean $pIC_{50}$ in molar (M) ±S.E.M for multiple assays of gemcitabine (C) and paclitaxel (D) in pancreatic cancer cell lines.

**Supplementary Figure 2.** Establishment of optimal conditions for measuring cell viability in a 3D monoculture model of Panc-1 or CAFs **(A)** Dose-response curves showing the response of PANC-1 cells cultured in 3D to gemcitabine using different cell numbers over a range of time-points to determine an optimal assay window. **(B)** Dose-response curves showing the response of CAFs (R3008) cultured at a variety of cell densities in 3D to gemcitabine treatment for 72h. Cell viability was determined using CellTiter-Glo at the specified time point and normalised to a DMSO control set to 100%.

**Supplementary Figure 3.** The addition of CAFs to a 3D co-culture model with pancreatic cancer cell lines impacts the efficacy of paclitaxel. Graphs show the comparison of a 2D standard monoculture cell viability assay, a 3D monoculture assay of pancreatic cancer cell lines and a 3D co-cultures assay of pancreatic cancer cell lines combined with CAFs, which were treated with various concentrations of paclitaxel. At 72h cell viability was determined using CellTiter-Glo. The data are shown as ±SD of one assay performed in triplicate and normalised to a DMSO control set to 100%.
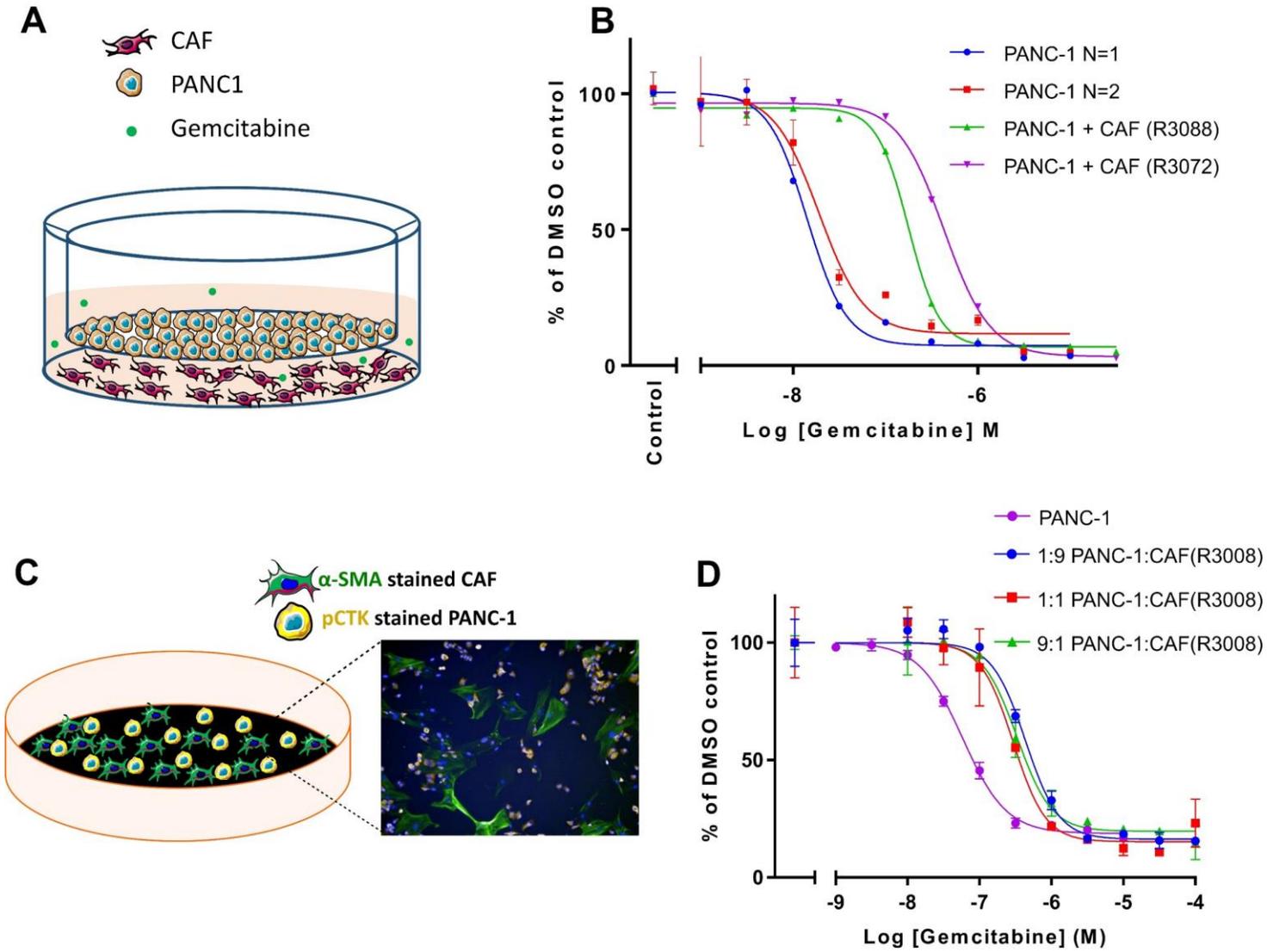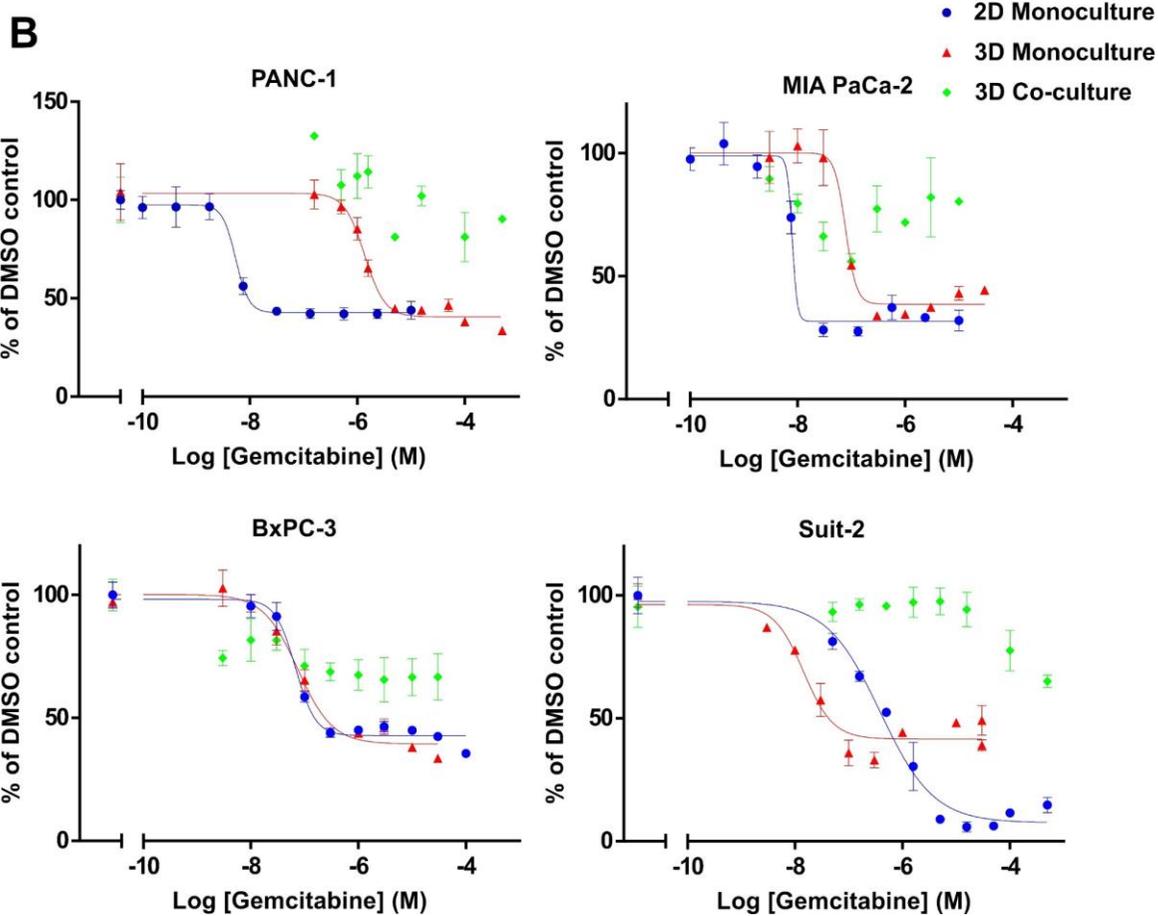
# Figure 1

# Figure 2

# Figure 3

**A**



**B**



**C**



**D**
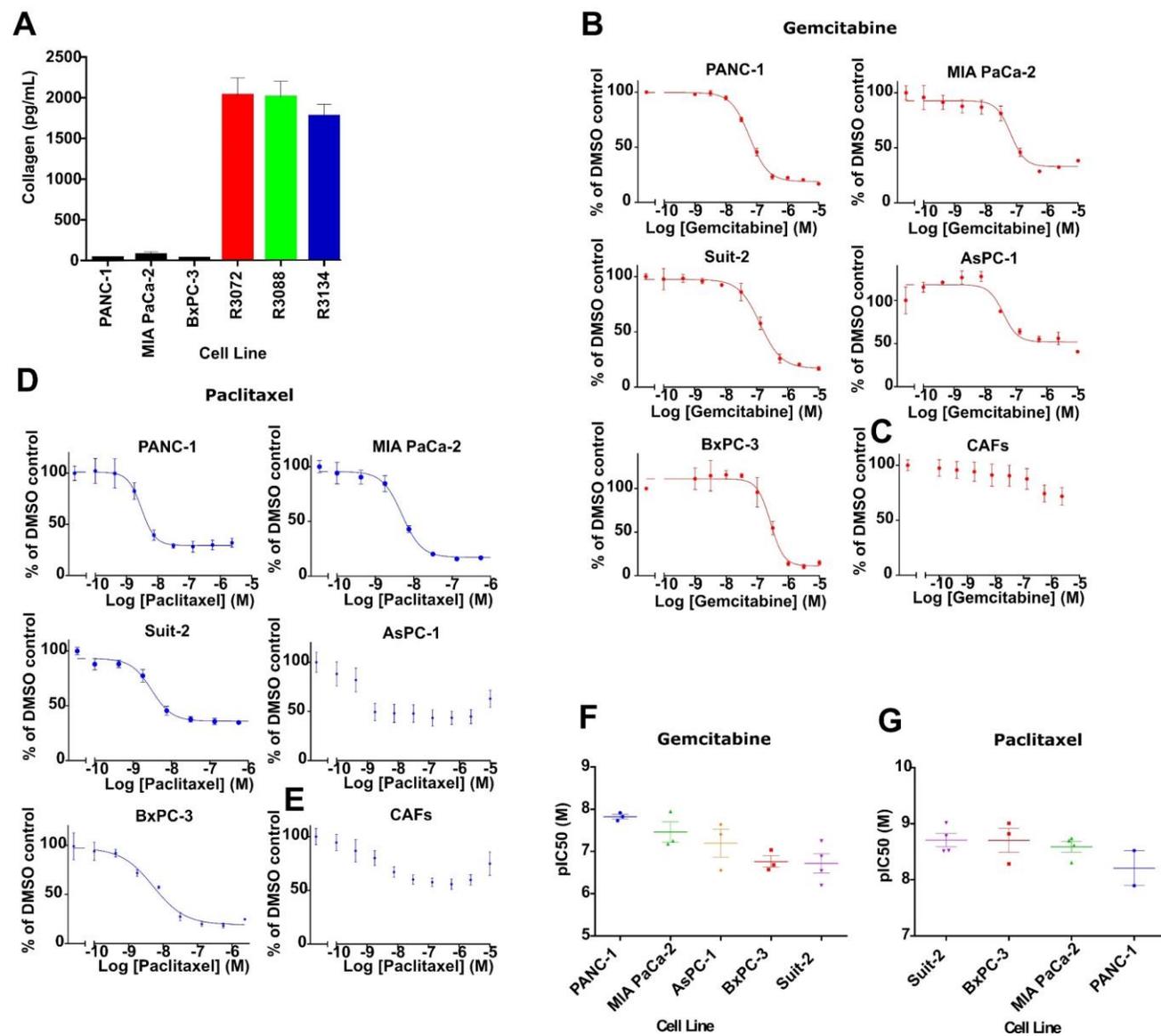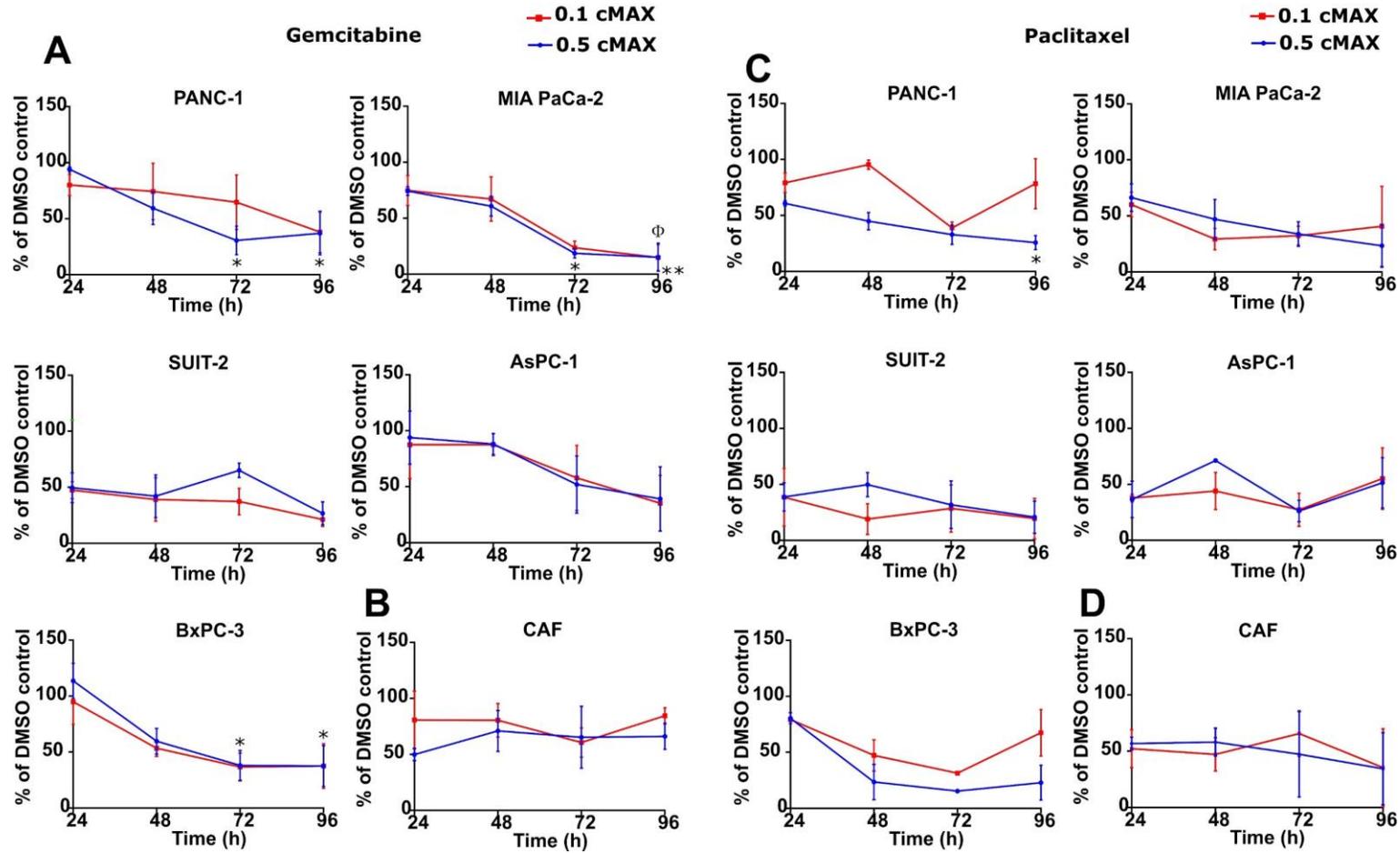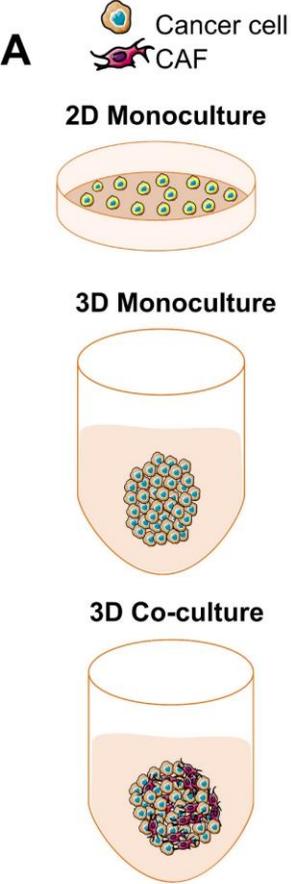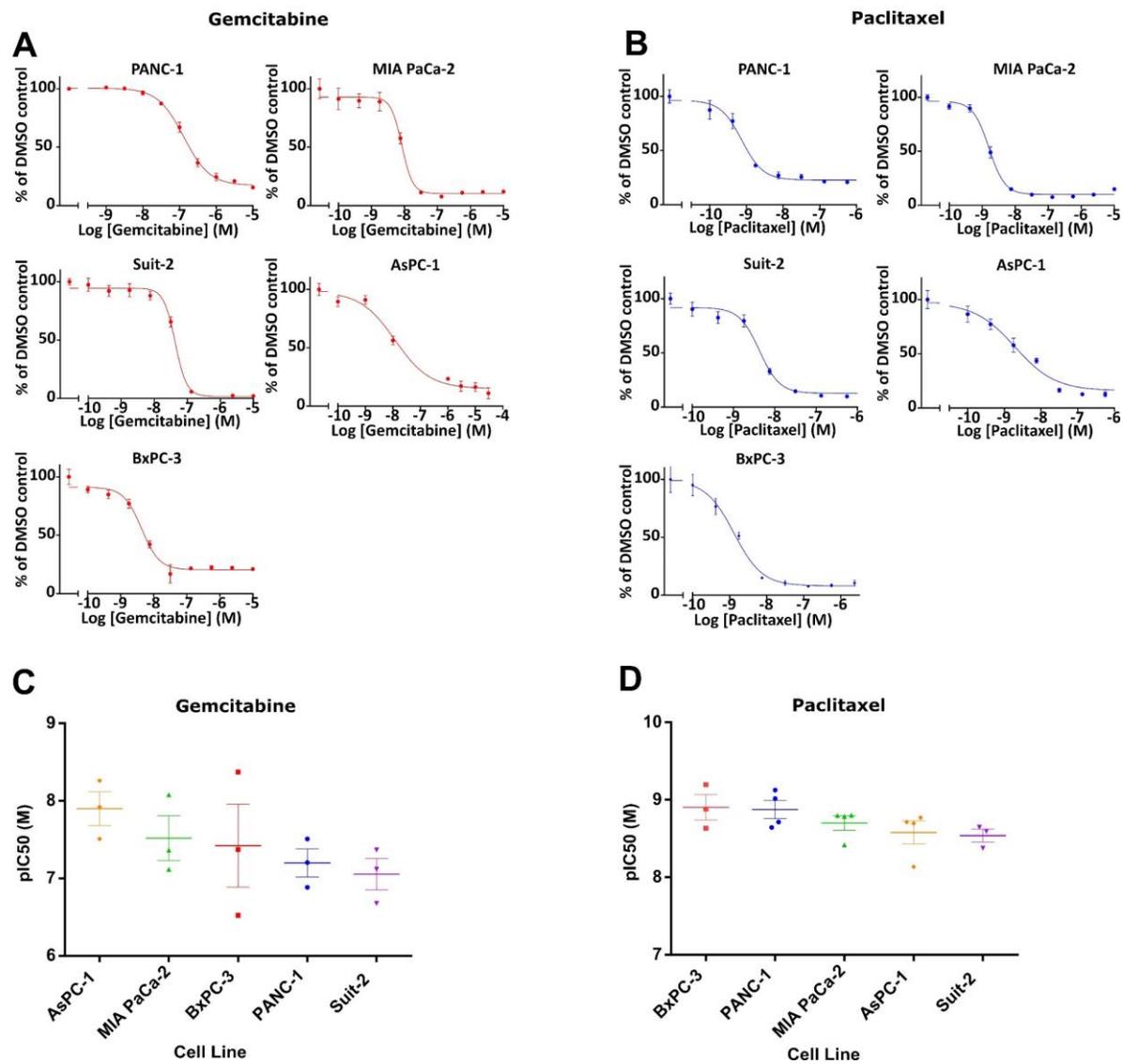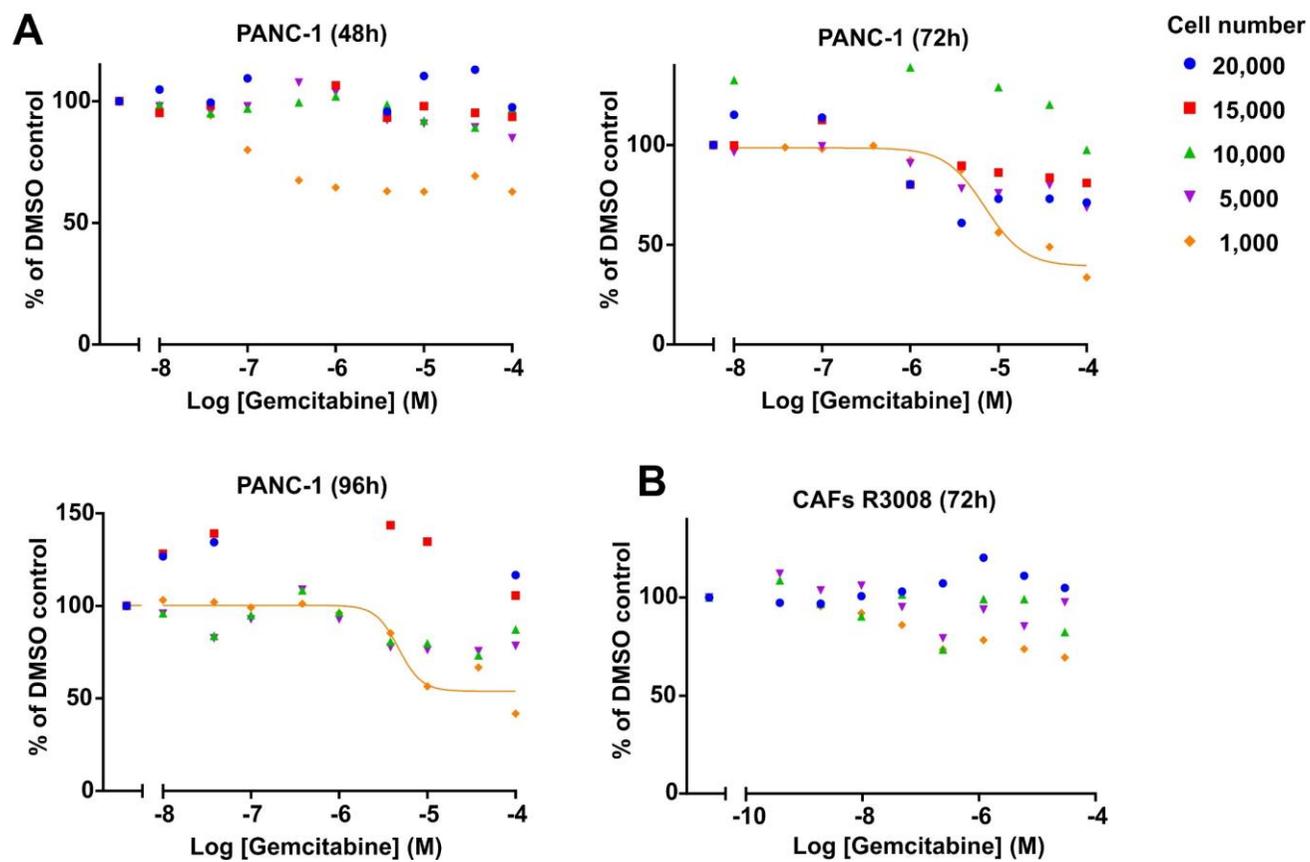
# Figure 4

# Supplementary Figure 1

## Supplementary Figure 2

# Supplementary Figure 3